Mass-spectrometric investigation of the stabilities and structures of Mn-O and Mn-Mg-O clusters

Paul J. Ziemann and A. W. Castleman, Jr.
Department of Chemistry, The Pennsylvania State University, University Park, Pennsylvania 16802
(Received 4 November 1991)

Time-of-flight mass spectrometry was used to investigate Mn-O and Mn-Mg-O clusters produced by a gas aggregation technique. The primary stoichiometries observed were $(MnO)_x^+$ ($x=1-13$) and $(MnO)_xO^+$ ($x=4-22$) clusters, and also these series with partial substitutions of Mg for Mn. The mass spectral abundance patterns suggest that the most stable structures for the stoichiometric clusters are stacks of rings composed of $(MnO)_3$ units, and that the oxygen-rich clusters prefer these structures with a single Mn atom vacancy. The partial substitution of Mg for Mn in the clusters appears to have little effect on these structural preferences. Interesting similarities and differences are observed when the stoichiometric and structural properties of these clusters are compared with the properties of the bulk materials, and also alkaline-earth oxide clusters.

I. INTRODUCTION

One area of cluster science that has received much attention in recent years is metal cluster chemistry,[1] since it is known that the activity of finely divided powders can be very different from the bulk. Investigators look with particular interest for size-specific cluster reactivity, and attempt to correlate observed patterns with structural or electronic properties.[2-4] These studies improve an understanding of chemisorption and the catalytic behavior of surfaces, and are particularly useful for comparison with the results of theoretical calculations, which often use a cluster to model the local interaction between the surface and adsorbate.

Somewhat surprisingly, there has been little study of metal oxide clusters, in spite of interest in the fundamental properties of the bulk systems, including high-temperature superconductivity and also the widespread use of metal oxides as catalysts, the importance of metal-oxygen chemistry in corrosion, and the use of these materials in high-temperature applications. Most investigations have focused on small clusters composed of a few tens of atoms,[5-8] although there have also been studied of larger clusters.[9-11]

Because of the paucity of information on such an important and potentially very interesting class of materials, we have recently commenced investigations of some relatively simple metal oxide compounds.[12-14] From experimental and theoretical studies of Mg-O and Ca-O clusters we obtained a variety of information on the structural, electronic, and fragmentation properties of these systems, and found that although Mg-O and Ca-O clusters have many properties in common, as one would expect since both metals are in the same group of the Periodic Table, they also exhibit interesting differences. There is still much to be learned from the study of these and other alkaline-earth oxides, but in an effort to enhance our understanding of oxides of electronically more complex metals we undertook an investigation of Mn-O clusters. The Mn-O system has an important similarity to the alkaline-earth oxides since, like them, crystalline MnO has the fcc structure. However, being a transition metal, Mn can exist in higher oxidation states than the alkaline-earth metals and can form oxides such as Mn_3O_4, Mn_2O_3, and MnO_2. The existence of systems with widely varying stoichiometries opens up the possibility of producing oxygen-rich clusters, which were never observed in our experiments with Mg or Ca. In addition to its value for making comparisons with the properties of Mg-O and Ca-O clusters, the Mn-O system is of interest in its own right. There have been recent studies of the electronic,[15,16] structural,[16,17] and chemical[18-20] properties of bulk MnO, and there is currently much interest in the role that Mn-O clusters play in photosynthesis.[21] In order to determine the extent to which different metal atoms can be interchanged in oxide clusters, and the degree to which this effects cluster structures, we have also produced mixed Mn-Mg-O clusters.

II. EXPERIMENT AND TECHNIQUE

The apparatus used in these experiments is shown in Fig. 1. Inside a liquid-nitrogen-cooled source chamber, Mn metal is evaporated from a boron nitride crucible that is resistively heated by a tungsten wire and heat shielded around the circumference and on the bottom by a tantalum sheet. The metal vapor is entrained in 2500–4000 sccm (standard cubic centimeter per minute) of cold He, whereupon Mn-O clusters are formed by reactions of the metal vapor with O_2 and/or H_2O which are present as contaminants in the carrier gas or enter the system through leaks. In some instances a few sccm of N_2O were also added to the source to shift the cluster distribution to larger sizes. Mixed Mn-Mg-O clusters are produced similarly, by adding a mixture of Mn and Mg chips to the crucible. The pressure in the source under these conditions is about 5 Torr, but the temperature in the crucible could not be measured because the upper

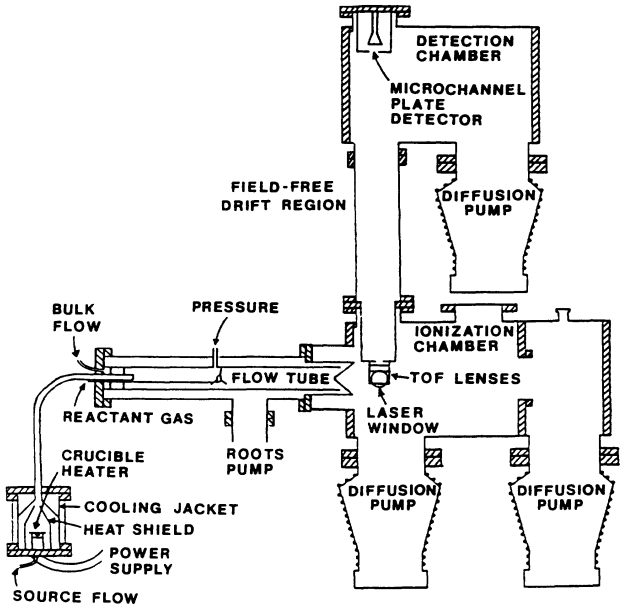

FIG. 1. Apparatus.

limit of the available thermocouple was about 1000 °C, which is well below the crucible temperature. The temperature is probably in the neighborhood of the melting point of Mn, which is 1244 °C. After leaving the source the clusters pass through a tube (75 cm long, 1.25 cm diameter) with a 90° bend in it, and into a flow tube (100 cm long, 6 cm diameter). Most of the gas is pumped away by a roots pump at the end of the flow tube, but a small fraction passes through an on-axis hole in a sampling cone and into the ionization region. The sampled flow tube effluent is then photoionized by a focused excimer laser beam and accelerated to about 2-kV energy in an electrostatic lens assembly, before entering a field-free drift region (75 cm) for time-of-flight mass analysis. Halfway along the drift tube an ion deflection unit, which is basically a pair of cylindrical plates with a pulsed potential across them (in this case 250 V and about 10–20 μs pulse width), deflects low-mass ions of high intensity that would otherwise saturate the detector and thereby reduce the signal intensity of clusters that arrive at later times. The undeflected ions are subsequently detected by a pair of microchannel plates and the resulting current is measured as a voltage drop across a 50-Ω impedance. This signal is fed into a 100-MHz transient recorder and signal averager, where it is digitized in 10-ns channels to produce a single spectrum, and then 100 spectra are averaged and transferred to a computer for display, storage, and handling. Typical laser powers, averaged over a 1-cm^2 iris through which the beam passes prior to entering the vacuum chamber, are about 10–50 mJ/pulse. Average power densities are about 0.3–1.5 MW/cm^2, but because the beam is focused they are much higher in the ionization region. The cluster mass spectra shown here were obtained by ionization at 248 nm, but experiments performed with 308-nm radiation yielded similar results. Fourier transform techniques were used to remove high-frequency noise from the mass spectra, and slightly sloping baselines were corrected by polynomial curve fitting. Great care was taken to ensure that none of these procedures had a significant effect on the cluster peak heights.

III. RESULTS AND DISCUSSION

A. Mn-O clusters

When pure Mn is evaporated from the crucible without the addition of an oxidant, Mn-O clusters dominate this mass spectrum, and the only unoxidized Mn species observed are Mn^+ ions. The hot Mn vapor is apparently so reactive that it is rapidly oxidized by trace quantities of O_2 and/or H_2O that leak into the system or enter with the He carrier gas. The formation of Mn-O clusters may occur through growth around a MnO molecule or other small seed, as appears to be the case for Mg-O and Ca-O clusters, or by the oxidiation of pure Mn clusters. Since the Mn_2 dimer is basically a van der Waals molecule[22] [the dissociation energy is about 0.3 eV (Ref. 23)], pure Mn clusters may be relatively unstable at the high source temperatures, and a Mn-O nucleus may be necessary for cluster formation.

Because it appears that an ionic model is inappropriate for Mn-O clusters (discussed below), we have not tried to make any calculations of the stabilites of these clusters, as we did for Mg-O clusters.[12] Instead, we have used ionic model calculations as a means to generate pictorial representations of the structures that we believe are most reasonable, based on the cluster abundance patterns. The structures shown here were obtained by allowing the clusters to relax from initial configurations composed of stacks of $(MnO)_3$ rings, with and without a Mn vacancy. The $(MnO)_{12}O^+$ calculation was started from a $3\times3\times3$ structure from which a central MnO molecule had been removed. The structure correspond to a local minima in the potential-energy surface, not the global minima which would be obtained if cubic structures were used for initial configurations. The calculations were performed by using the single charges and parameters used previously for Mg-O clusters.

Because of the possibility that hydrogen from H_2O contamination could be present in the clusters, we carefully calibrated the mass spectrometer over the entire Mn-O cluster mass range, and feel quite certain that the peaks we observe contain little, if any, contribution from hydrogen. Furthermore, we note that when N_2O was added in great excess of any H_2O which might have been present, many larger cluster peaks appeared in the mass spectrum, but no significant change occurred in the original peaks as might be expected if the clusters contained less hydrogen as a result of N_2O replacing H_2O as an oxidant. In the absence of N_2O, clusters are most likely formed through reactions of metal with O_2, or by reactions with H_2O in which H_2 is lost.

A typical mass spectrum from these experiments is shown in Fig. 2, in which the primary series of peaks corresponds to $(MnO)_x^+$ clusters with $x=1-13$. A relatively intense series of $(MnO)_xO^+$ clusters is also observed, as

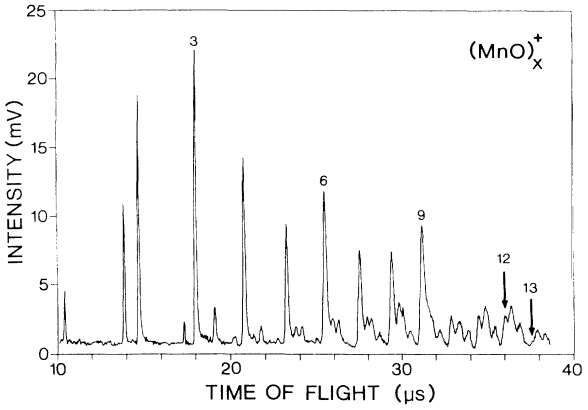

FIG. 2. Time-of-flight mass spectrum of $(MnO)_x^+$ clusters. The magic numbers and the upper limit of the distribution, $(MnO)_{13}^+$, are numbered. The peaks immediately to the right of $(MnO)_x^+$ peaks correspond to $(MnO)_xO^+$ clusters, and are shown more clearly in Fig. 3. The peaks next to $(MnO)_xO^+$ cluster peaks are due to a contaminant (see text for details).

well as low intensities [except for the large $(MnO)Mn^+$ peak] of $(MnO)_xMn^+$ and $(MnO)_xA^+$ clusters, where A is a contaminant with a mass close to 27 amu. We suspect that the contaminant is BO (26.8 amu) which comes from a reaction of oxygen with the BN crucible, since these peaks are absent when an Al_2O_3 crucible is used. The $(MnO)_xO^+$ clusters are more abundant than $(MnO)_x^+$ clusters for $x > 10$, and an expanded mass spectrum of these is shown in Fig. 3 for $x = 4-22$. When this spectrum was obtained, Mg was also present in the crucible and a trace of N_2O was added to the source to generate the large clusters. But, similar distributions of $(MnO)_xO^+$ clusters (of smaller maximum size) have been observed by using pure Mn and no N_2O.

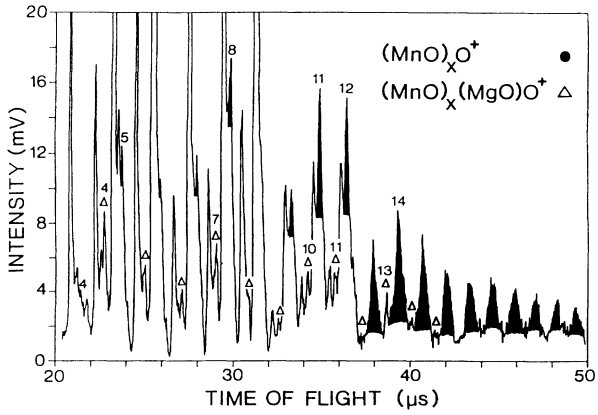

FIG. 3. Time-of-flight mass spectrum of $(MnO)_xO^+$ and $(MnO)_x(MgO)O^+$ clusters. The magic numbers in the distributions are numbered, as are the large peaks due to $(MnO)_{12}O^+$ and $(MnO)_{11}(MgO)O^+$. The unlabeled open peaks correspond to $(MnO)_x^+$ or $(MnO)_x(MgO)_y^+$ clusters, and are shown more clearly in Figs. 2 and 4.

The abundance patterns of both $(MnO)_x^+$ and $(MnO)_xO^+$ clusters exhibit local maxima which we interpret as being indicative of the relative stabilities of the cluster ions.[24–26] When the clusters are in the ionization region they can be heated to relatively high temperatures by the absorption of multiple photons, and subsequently lose this excess energy by ionization and evaporation. As a result of this process, cluster ions which are more stable than their neighbors obtain enhanced relative abundances. In Fig. 2, the magic numbers for $(MnO)_x^+$ clusters appear at $x = 3$, 6, 9, and 12. However, the $(MnO)_2^+$ peak is also quite large, and under some conditions may become comparable in intensity to $(MnO)_3^+$. In Fig. 3, the magic numbers of $(MnO)_xO^+$ clusters appear at $x = 5$, 8, 11 (12 is almost as large), and 14.

The abundance patterns in these two cluster series are similar to, but different in a few significant ways, from those observed for Mg-O and Ca-O clusters.[6,7,11–14] The major difference between the mass spectra of the stoichiometric Mn and alkaline-earth oxide clusters is that a magic number appears at $(MnO)_3^+$, rather than at $(MnO)_2^+$ and $(MnO)_4^+$. In the mass spectra of $(MgO)_xMg^+$ and $(CaO)_xCa^+$ clusters, maxima are observed at $x = 5$, 8, 11, and 13, and at $(CaO)_3Ca^+$. The abundance patterns of the $(MnO)_xO^+$ clusters, which have an excess O atom rather than a metal atom, differ from these in that a magic number appears at $(MnO)_{14}O^+$ instead of at $(MnO)_{13}O^+$, the intensity of the $(MnO)_{12}O^+$ peak is almost the same as that of $(MnO)_{11}O^+$, and whereas there is no minimum size for $(MgO)_xMg^+$ and $(CaO)_xCa^+$ clusters, no $(MnO)_xO^+$ clusters are observed for $x < 4$.

The magic numbers observed for $(MnO)_x^+$ and $(MnO)_xO^+$ clusters can be explained in terms of the exceptional stabilities of certain cluster geometries. Whereas these assignments are not definitive, we believe they provide a consistent explanation of the data. For $(MnO)_x^+$ clusters, the maxima at $x = 3$, 6, 9, and 12 suggest that the preferred structures are those generated by stacking hexagonal $(MnO)_3$ rings on top of each other. These structures are shown at the top of Fig. 4. The rings are joined together by square $(MnO)_2$ units, whose stability is also reflected in the high intensity of $(MnO)_2^+$ in the mass spectrum. Unlike $(MgO)_x^+$ and $(CaO)_x^+$ clusters, whose magic numbers at $x = 2$ (square) and 4 (cube) indicate that cubic structures are the most stable for those systems even at the smallest sizes, $(MnO)_x^+$ clusters appear to have noncubic structures. This is in spite of the fact that, like MgO and CaO, bulk solid MnO has the fcc crystal structure.

It is apparent that the presence of magic numbers at $x = 6$, 9, and 12 for both $(MnO)_x^+$ and $(MgO)_x^+$ and $(CaO)_x^+$ clusters lends some uncertainty to our assignment of different structures to these systems. Although the maximum at $(MnO)_3^+$ suggests that the larger $(MnO)_x^+$ clusters preferentially form stacks of hexagonal rings, we cannot be certain that the stacked rings do not contract to form 3×2 rectangles, resulting in $3\times2\times2$, $3\times2\times3$, and $3\times2\times3$ cuboids. Fortunately, the abundance patterns observed for $(MnO)_xO^+$ clusters provide

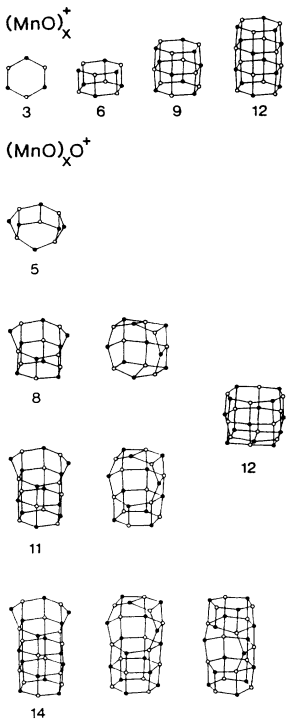

FIG. 4. Proposed structures of $(MnO)_x^+$ and $(MnO)_xO^+$ clusters, based on the magic numbers observed in mass spectra.

additional information on structural stabilities. The key feature in the spectrum in Fig. 3 is that the peak at $(MnO)_{13}O^+$ is a local minimum, rather than a maximum, as observed in the mass spectra of singly and doubly charged $(MgO)_xMg$ and $(CaO)_xCa$ clusters and in almost all the nonstoichiometric alkali halide clusters [the only exception is $(NaI)_xI^-$];[27] it is always attributed to the exceptional stability of the $3\times3\times3$ cuboid structure. The absence of a magic number at $(MnO)_{13}O^+$ suggests that $(MnO)_xO^+$ clusters prefer noncubic structures. Assuming this is the case, the abundance patterns observed for $(MnO)_xO^+$ clusters can be explained in terms of the exceptional stabilities of the structures shown in Fig. 4. The structures assigned to $x=5$, 8, 11, and 14 can be generated from stacks of 2, 3, 4, and 5 $(MnO)_3$ rings, respectively, by removing a Mn atom from each of the nonequivalent sites in the cluster. The structure shown for $(MnO)_{12}O^+$ can be generated by the addition of a $(MnO)_4$ ring to the second $(MnO)_8O^+$ structure. The resultant structure is essentially a $3\times3\times3$ cube with a MnO molecule removed. It is also worth noting that by removing a Mn atom from the structure proposed for $(MnO)_5O^+$, the cluster can easily distort into an adamantanelike structure which has been observed for $(MnO)_4O_2$ in solution studies[28] and has been suggested as an intermediate in the mechanism of photosynthetic O_2 evolution.[29] Rather than forming compact cubic structures by combining square units, these clusters apparently form structures which are combinations of squares, hexagons, and an occasional octagon.

The simplest explanation of why Mn-O clusters have noncubic structure, whereas Mg-O and Ca-O clusters have cubic structures, is that the presence of *d* electrons in Mn atoms allows them to undergo more metal-metal bonding than can alkaline-earth metal atoms, and this results in a difference in structural preferences. In a $(MO)_3$ cluster (*M* denotes a metal atom) with a perfect 3×2 rectangular structure, the length (*r*) of two of the *M*-*M* bonds is $r(M\text{-}M)=\sqrt{2}\times r(M\text{-}O)$ and the length of the other is $r(M\text{-}M)=2\times r(M\text{-}O)$, whereas for a hexagon the *M*-*M* and *M*-O bond lengths are the same. It may therefore be energetically favorable for Mn-O clusters to form hexagonal rings which have six Mn-O bonds and three Mn-Mn bonds, rather than 3×2 rectangles with seven Mn-O bonds and three much weaker Mn-Mn bonds.

Although differences in bond character may account for the greater stabilities of stacked-ring structures (with and without Mn vacancies) compared to cubic structures, the bonding in Mn-O clusters may not be different enough from that in Mg-O and Ca-O clusters (indicated from studies of the bulk[30–33]) to explain the low stability of a $3\times3\times3$ structure for $(MnO)_{13}O^+$. Instead, this structure may be less stable for $(MnO)_{13}O^+$ than it is for either $(MgO)_{13}Mg^+$ or $(CaO)_{13}Ca^+$ because higher charges on the metal atoms in the oxygen-rich clusters (assuming oxygen has the same charge in the Mg-O, Ca-O, and Mn-O systems) destabilizes the compact cubic structure.

Another interesting feature in the mass spectra is the increase with increasing cluster size in the intensities of $(MnO)_xO^+$ clusters relative to $(MnO)_x^+$ clusters, and the eventual disappearance of the latter beyond about $(MnO)_{13}^+$ (Figs. 2 and 3). It is known from solid-state studies that MnO can accommodate up to about 10% excess O atoms before another structure begins to form,[34,35] and that up to this point the O atoms are accomodated by the formation of isolated Mn vacancies in the fcc lattice (rather than as interstitial O atoms).[36] The patterns of $(MnO)_x^+$ and $(MnO)_xO^+$ cluster abundances suggest that excess O atoms are also incorporated into the lattice of the small clusters through the formation of Mn vacancies, although the structures are distorted from those of the bulk. Furthermore, the smallest $(MnO)_xO^+$ cluster observed in the mass spectrum is $(MnO)_4O^+$, suggesting that clusters containing more than about 20% excess O atoms are unstable. This critical composition is not too different from the bulk value of about 10%, and it may be that the factors responsible for the absence of small $(MnO)_xO^+$ clusters are related to those which destabilize the solid.

The mass spectra of Mn-O clusters are similar in a number of ways to spectra obtained for Fe-O clusters produced by laser vaporization.[37] In those studies, $(FeO)_x^+$ clusters are observed from $x=1$ to about $x=16$ [$x=1-13$ for $(MnO)_x^+$ clusters], and $(FeO)_xO^+$ clusters first appear at $x=3$[$x=4$ for $(MnO)_xO^+$ clusters] and then increase in intensity with increasing cluster size until they become more abundant than the stoichiometric clusters for $x\geq10$ [$x\geq11$ for $(MnO)_xO^+$ and $(MnO)_x^+$ clusters]. The mass spectra of the two systems differ in that, whereas Mn-O clusters are only observed with up to

one excess O atom, many Fe-O clusters have more than one and, beyond about $x=18$, the latter clusters are the most abundant. But more importantly, although magic numbers are present in Mn-O cluster distributions, almost none are observed in the mass spectra of Fe-O clusters [the peak corresponding to $(FeO)_3^+$ appears to be a magic number, but this is not mentioned in the paper]. The similarities in the stoichiometries of Mn-O and Fe-O clusters are not surprising since, like MnO, bulk FeO has a fcc structure that can accommodate up to about 10–15% excess O atoms.[38] The discrepancies in the mass spectra are more difficult to explain, but they may be related to the properties of the bulk materials which stabilize the formation of isolated Mn vacancies in solid MnO (Ref. 36) while leading to aggregated Fe vacancies in FeO.[39,40]

B. Mn-Mg-O clusters

The abundance patterns of $(MnO)_x^+$ and $(MnO)_xO^+$ clusters are essentially unchanged by the substitution of Mg for Mn in the cluster lattice. This can be seen most clearly for the $(MnO)_xO^+$ and $(MnO)_x(MgO)O^+$ clusters shown in Fig. 3. The distribution of $(MnO)_x(MgO)O^+$ clusters is nearly identical (within a scale factor) to that of $(MnO)_xO^+$ clusters, although it is shifted to the left by one MnO unit due to the presence of a MgO molecule. Similar behavior is observed for the $(MnO)_x(MgO)_y^+$ clusters shown in Fig. 5, although it is less obvious due to the greater variety of cluster compositions. Starting with the series of pure $(MnO)_x^+$ clusters [i.e., the peaks labeled $(x,0)$], maxima occur at (6,0) and (9,0), which are the same as those observed when only Mn is evaporated from the crucible. Similarly, in any cluster series obtained by increasing x or y alone, maxima occur when $x+y=6$ or 9 (in some cases, the cluster following a maxima in a particular series is too small to be observed). In addition, there are three large peaks at (8,4), (9,3), and (10,2), such that $x+y=12$, whereas peaks with $x+y=11$ or 13 are lost in the noise. Note that the $(MnO)_{12}^+$ cluster is also exceptionally stable in the pure Mn-O spectrum.

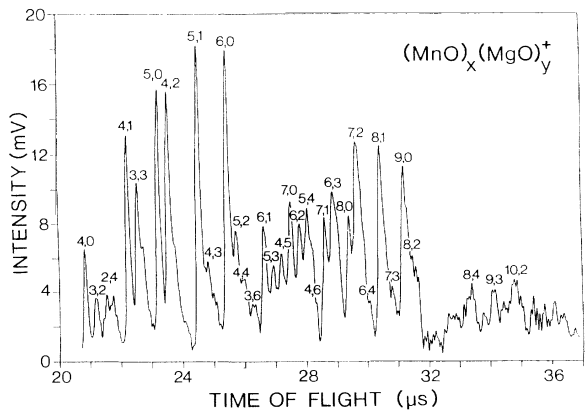

FIG. 5. Time-of-flight mass spectrum of $(MnO)_x(MgO)_y^+$ clusters.

It is perhaps not surprising that the magic numbers in the $(MnO)_x^+$ cluster distribution are unaffected by the substitution of Mg, since over the size range examined these are the same magic numbers observed for $(MgO)_x^+$ clusters. We would like to know the distribution of mixed clusters with $x+y<5$, in which range pure $(MnO)_x^+$ and $(MgO)_x^+$ cluster distributions exhibit different magic numbers. Unfortunately, during the experiment when these spectra were collected, the ion deflection unit was set to deflect clusters smaller than about 250 amu, due to the presence of a large background pump oil signal. The mixed clusters were observed in only a few of the mass spectra, near the end of the experiment when the crucible was almost empty. Additional attempts to produce the mixed clusters failed, as only Mg-O clusters followed by Mn-O clusters were observed. Apparently all the Mg evaporates before a temperature can be reached at which sufficient Mn will also evaporate. In the one successful experiment, the mixed clusters probably came from the evaporation of an oxide-coated piece of Mg that managed to survive until Mn vapor was also present.

The ease of substitution of Mg for Mn in Mn-O clusters is predictable, based on the results of solid-state studies.[41] The most important criterion for forming completely miscible solid solutions is that the end members have the same structure, and solid MnO and MgO are both fcc. In such isostructural systems, the most important determinant of solubility is the similarity in the sizes of the ions being mixed. Since the metal-oxygen bond lengths (for this comparison these are a better measure of ion size than standard ionic radii, which are averages for a variety of compounds) of MnO and MgO are 2.2 and 2.1 Å, respectively,[42] high solubility can be expected. This prediction is born out by investigations of solid solutions of MnO and MgO, in which complete miscibility is observed over the entire range of compositions.[43–45] Mixing could be even easier for the clusters, which can undergo distortions more easily than the bulk in order to accommodate ions of different sizes. However, the possibility must also be considered that the sizes of the Mg and Mn ions in the clusters could be different from those in the bulk, and that mixing in the clusters could be hindered as a result. Since the bond distances of the MnO and MgO molecules are 1.77 and 1.75 Å,[46] respectively, this is not an issue. We do not observe a complete mixing series in the cluster mass spectra, but for $x+y=6$ the range from (6,0) to (2,4) is present, as is the range from (9,0) to (3,6) for $x+y=9$. These series only span the range of compositions from 0% to 67% Mg, but if we had more control over the composition of the metal vapor in the source it is likely that the entire range could be covered.

IV. CONCLUSIONS

The abundance patterns observed in the mass spectra of $(MnO)_x^+$ and $(MnO)_xO^+$ clusters can be explained in terms of the exceptional stabilities of certain cluster structures. The most stable structures for $(MnO)_x^+$ clusters appear to be composed of stacks of hexagonal

$(MnO)_3$ rings, whereas the $(MnO)_xO^+$ clusters prefer these with a Mn vacancy. The structures are different from the cubic ones formed by Mg-O and Ca-O clusters, in spite of the fact that bulk solid MnO, MgO, and CaO are all fcc crystals. The formation of Mn vacancies in oxygen-rich clusters is similar to the behavior of bulk MnO when excess O atoms are introduced into the fcc lattice, although the structures of the vacancy sites are different. One of the most obvious discrepancies between the mass spectra of Mn-O and alkaline-earth oxide clusters is that no magic number appears at $(MnO)_{13}O^+$, indicating that the $3\times3\times3$ cubic which is so stable for $(MgO)_{13}Mg^+$ and $(CaO)_{13}Ca^+$ clusters (as well as the alkali halides) is not particularly stable for this cluster. The differences is the structures of Mn-O clusters, compared to Mg-O and Ca-O clusters, may be due to stronger metal-metal bonding by *d* electrons in Mn-O clusters. For the nonstoichiometric clusters the differences could also result from the opposite effects that an excess O atom and an excess metal atom have on the charges on metal ions in a cluster, which in turn affect the cluster structure.

The magic numbers observed in the mass spectra of mixed Mn-Mg-O clusters are the same as those of pure Mn-O clusters, indicating that the structures are not significantly altered by the substitution of Mg for Mn in the cluster lattice. The complete miscibility observed for solid solutions of MnO and MgO appears to also hold for the clusters, although we could not investigate the very small cluster sizes where differences would be most obvious.

ACKNOWLEDGMENTS

We gratefully acknowledge the E. I. DuPont de NeMours & Company for financial support. The authors also thank Dr. Yasihiro Yamada and Dr. Andreas Hartmann for helpful discussions during the course of this work.

[1]A. Kaldor, D. M. Cox, and M. R. Zakin, in Adv. Chem. Phys. **70**, 211 (1988).
[2]R. L. Whetten, D. M. Cox, D. J. Trevor, and A. Kaldor, Phys. Rev. Lett. **54**, 1494 (1985).
[3]W. F. Hoffman III, E. K. Parks, G. C. Neiman, L. G. Pobo, and S. J. Riley, Z. Phys. D **7**, 83 (1987).
[4]R. E. Leuchtner, A. C. Harms, and A. W. Castleman, Jr., J. Chem. Phys. **91**, 2753 (1989).
[5]R. B. Freas, B. I. Dunlap, B. A. Waite, and J. E. Campana, J. Chem. Phys. **86**, 1276 (1987).
[6]W. A. Saunders, Phys. Rev. B **37**, 6583 (1988).
[7]W. A. Saunders, Z. Phys. D **12**, 601 (1989).
[8]W. Yu and R. B. Freas, J. Am. Chem. Soc. **112**, 7126 (1990).
[9]G. C. Nieman, E. K. Parks, S. C. Richtsmeier, K. Liu, L. G. Pobo, and S. J. Riley, High Temp. Sci. **22**, 115 (1986).
[10]T. P. Martin and T. Bergmann, J. Chem. Phys. **90**, 6664 (1989).
[11]I. Katakuse, T. Ichihara, H. Ito, and M. Hirai, Mass Spectrom. **1**, 16 (1990).
[12]P. J. Ziemann and A. W. Castleman, Jr., J. Chem. Phys. **94**, 718 (1991).
[13]P. J. Ziemann and A. W. Castleman, Jr., Phys. Rev. B **44**, 6488 (1991).
[14]P. J. Ziemann and A. W. Castleman, Jr., J. Phys. Chem. **96**, 4271 (1992).
[15]A. Fujimori, N. Kimizuka, T. Akahane, T. Chiba, S. Kimura, F. Minami, K. Siratori, M. Taniguchi, S. Ogawa, and S. Suga, Phys. Rev. B **42**, 7580 (1990).
[16]R. B. Grimes and D. Onwood, J. Chem. Soc. Faraday Trans. **86**, 233 (1990).
[17]M. A. Langell and N. R. Cameron, Surf. Sci. **185**, 105 (1987).
[18]R. S. Murthy, P. Patnaik, P. Sideswarah, and J. Jayamani, J. Catal. **109**, 298 (1988).
[19]K. M. Kreitman, B. Baerns, and J. B. Butt, J. Catal. **105**, 319 (1987).
[20]V. M. Allen, W. E. Jones, and P. D. Pacey, Surf. Sci. **199**, 309 (1988).
[21]G. W. Brudvig and R. H. Crabtree, in *Progress in Inorganic Chemistry,* edited by S. J. Lippard (Wiley, New York, 1989), Vol. 37, pp. 99–143.
[22]C. A. Baumann, R. J. Van Zee, S. V. Bhat, and W. Weltner, Jr., J. Chem. Phys. **78**, 190 (1983).
[23]K. Ervin, S. K. Loh, N. Aristov, and P. B. Armentrout, J. Phys. Chem. **87**, 3593 (1983).
[24]T. P. Martin, Phys. Rep. **95**, 167 (1983).
[25]T. D. Märk and A. W. Castleman, Jr., Ad. At. Mol. Phys. **20**, 65 (1985).
[26]A. W. Castleman, Jr. and R. G. Keesee, Ann. Rev. Phys. Chem. **37**, 525 (1986).
[27]Y. J. Twu, C. W. S. Conover, Y. A. Yang, and L. A. Bloomfield, Phys. Rev. B **42**, 5306 (1990).
[28]K. Weighardt, U. Bossek, and W. Gebert, Agnew, Chem. Int. Ed. Engl. **22**, 328 (1983).
[29]G. W. Brudvig and R. H. Crabtree, Proc. Natl. Acad. Sci. USA **83**, 4586 (1986).
[30]S. Sasaki, K. Fujino, and Y. Takeuchi, Proc. Jap. Acad. **55B**, 43 (1979).
[31]J. H. Binks and J. A. Duffy, J. Solid State Chem. **87**, 195 (1990).
[32]B. F. Levine, Phys. Rev. B **7**, 2591 (1973).
[33]B. F. Levine, J. Chem. Phys. **59**, 1463 (1973).
[34]T. E. Moore, M. Ellis, and P. W. Selwood, J. Am. Chem. Soc. **72**, 856 (1950).
[35]M. Keller and R. Deickmann, Ber. Bunsenges. Phys. Chem. **89**, 883 (1985).
[36]D. Schuster, R. Dieckmann, and W. Schweika, Ber. Bunsenges. Phys. Chem. **93**, 1347 (1989).
[37]S. J. Riley, E. K. Parks, G. C. Nieman, L. G. Pobo, and S. Wexler, J. Chem. Phys. **80**, 1360 (1984).
[38]P. Kofstad, *Nonstoichiometry, Diffusion, and Electrical Conductivity in Binary Metal Oxides* (Wiley, New York, 1972), p. 221.
[39]W. K. Chen and N. L. Peterson, J. Phys. Chem. Solids **36**, 1097 (1975).
[40]C. R. A. Catlow and A. M. Stoneham, J. Am. Ceram. Soc. **64**, 234 (1981).
[41]P. K. Davies and A. Navrotsky, J. Solid State Chem. **46**, 1 (1983).

[42]*CRC Handbook of Chemistry and Physics,* 63rd ed., edited by R. C. Weast and M. J. Astle (CRC, Boca Raton, 1982).
[43]E. Woermann and A. Muan, Mater. Res. Bull. **5**, 779 (1970).
[44]W. C. Hahn, Jr. and A. Muan, Mater. Res. Bull. **5**, 955 (1970).
[45]S. Raghavan, G. N. K. Iyengar, and K. P. Abraham, J. Chem. Thermodyn. **17**, 585 (1985).
[46]K. P. Huber and G. Herzberg, *Molecular Spectra and Molecular Structure IV. Constants of Diatomic Molecules* (Van Nostrand Reinhold, New York, 1979).